MODEL PROBLEMS FOR FISH SCHOOLING

SILAS ALBEN*

Abstract. We review recent work on model systems for body-vortex and body-body interactions in a fluid, related to fish schooling. The studies show a variety of structured and disordered dynamics which can occur when vortices interact with passive and actively-driven deformable bodies. The energy savings due to body-vortex interactions depend strongly on the geometric arrangement of multiple bodies and/or ambient vortices, the phases of the bodies' motions relative to those of the vortices and other bodies, and the rigidity of flexible appendages.

Key words. Flexible, vorticity, coupled, flow-body.

AMS(MOS) subject classifications. 76Z10, 74F10, 74L15, 92C10.

1. Introduction. This article reviews a collection of recent model problems which address different aspects of fish schooling. We focus on theoretical work, and the experiments which were their direct inspiration. In most cases the experiments can also be considered physical/biological models (in the sense of [1]) for the complicated phenomena of fish schooling. In particular, the experiments and theories described here mainly focus on the interactions of individual bodies with ambient vorticity, or two bodies coupled to each other through their shared fluid environment. Model "swimmers" such as rigid foils, passive elastic rods, or isolated fins driven at the leading edge, yield simpler problems which can be analyzed. Thus important phenomena can be studied without the full complexity of real fish.

2. Bodies interacting with vorticity. Even though many aspects of thrust generation by individual flexible bodies remain mysterious, a number of recent studies have considered how multiple flexible bodies interact with each other through a fluid. The interaction occurs principally through vorticity that is shed from the edges of these bodies, and then collides with other bodies downstream. Thus a useful precursor to the problem of fish schooling is the study of how bodies interact with ambient vorticity.

The experiment of Liao *et al.* [2] increased interest in this field by showing how a single swimming trout alters its swimming motion in the presence of vorticity. When a D-shaped cylinder was placed in a steady flow, a "von Kármán" street of concentrated vortices of alternating sign was shed from the two sides of the cylinder. When placed in this vortex-street wake, the trout was able to hold its position in the flow with less energy, compared to the same flow situation without the upstream cylinder.

* School of Mathematics, Georgia Institute of Technology, Atlanta, GA 30332 (alben@math.gatech.edu). This work was supported by NSF-DMS 0810602 and 1022619.

The trout altered its usual swimming motion to increase its side-to-side motion, increasing its ability to interact with the vortices. The vortices emerged from this interaction significantly weakened, indicating that the trout had extracted significant kinetic energy from the vortices. The usual pattern of muscular contraction all along the trout body, in the absence of the cylinder, was replaced by a contraction concentrated in the upstream portion of the body. The remainder of the body was thereby left to interact with vortices more like a passive flexible element. Liao also reviewed the experimental literature on more general cases of swimming in turbulent flows [3–5].

An earlier theoretical study by Streitlien *et al.* [6] studied the motion of a rigid body in an array of point vortices, and found significant gains in propulsive efficiency due to the interaction of the body with the point vortices. However, no optimal motion could be identified, since the efficiency became arbitrarily large as the body became closer to the point-vortex singularities. In real flows, the vortices themselves deform significantly upon encountering a body, and their subsequent dynamics can depend sensitively on their spatial structure [7].

In [8], we considered a periodic flexible sheet swimming along the midline of a von Kármán street. The model is somewhat similar to Taylor's infinite swimming sheet at low Reynolds number [9]. In our work, the Reynolds number is large, and the flow can be solved analytically for small sheet deflections by posing a periodic vortex sheet along the swimming body. The body does not swim freely, but instead deforms transversely to itself, in a traveling wave which moves with the vortex street, in order to maximize the upstream thrust force acting on it. The optimal solutions are shown in Figure 1a. When the vortex street width d is large relative to its streamwise periodic length l, shown schematically by the solid-line vortices, the optimal swimming shape is sinusoidal, also shown by a solid line. In the other limit, when the vortex street is narrow (d/l is small), shown by the dotted-line vortices, the optimal swimming shape consists of sharp peaks near the vortices, also shown by a dotted line. An intermediate case is shown for comparison. In all cases, the sheet has maximum slope adjacent to the vortices, which allows the pressure force from the vortices to act mostly in the upstream direction.

The analytical solutions yield closed formulae for the output power P_{out} on the sheet, per unit period length. P_{out} is the product of thrust force with the mean flow speed that the body encounters U, and is nondimensionalized by a product of the fluid area density ρ_f, the amplitude of the traveling wave A, the square of the strength of the vortices in the street Γ, and U. Figure 1b shows the output power for the full range of vortex street width parameter d/l. For narrow vortex streets, the output power diverges as a power law, $\sim (d/l)^{-5/2}$, while for wide vortex streets the output power decays exponentially, $\sim e^{-d/l}$. Wide vortex streets have an

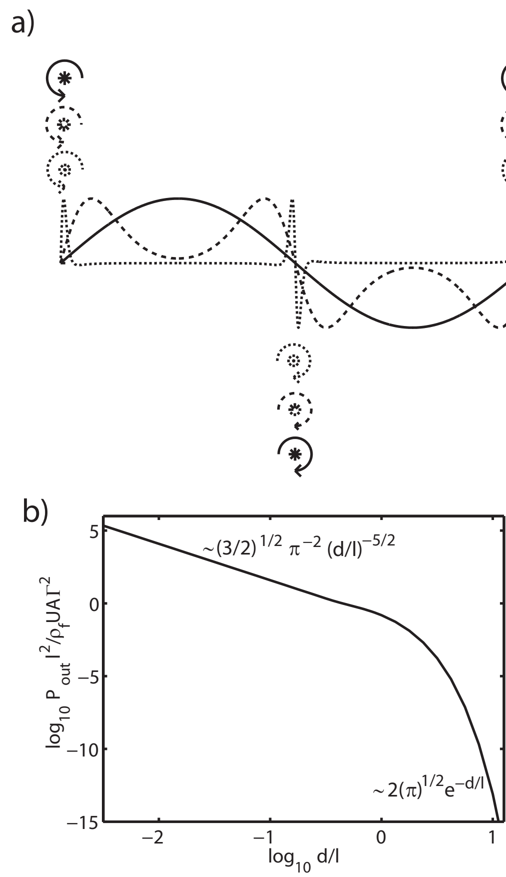

FIG. 1. *a, Thrust-maximizing motions of a periodic swimming sheet immersed in a vortex street when the vortex street width is large (solid line), moderate (dashed line), and small (dotted line). b, The output power P_{out}, nondimensionalized, versus the vortex street aspect ratio d/l. Adapted from [8].*

exponentially small central flow, so little pressure is induced on a body in the center of the vortex street.

The periodic model in [8] is also reasonable for a body of finite length, when the body is long relative to the streamwise spacing between the vortices. In this case the trailing edge wake has relatively weak vorticity [10]. Excitation of passive bodies by vortices were studied in [11, 12]. More general cases of *finite* swimming bodies in a von Kármán street were studied in [10]. The study considered only relatively wide vortex streets, which are only slightly perturbed by the body's presence. This regime also simplifies the trailing vortex wake to one which is approximately straight, and with a sinusoidal-traveling-wave distribution of vorticity. In this case the entire

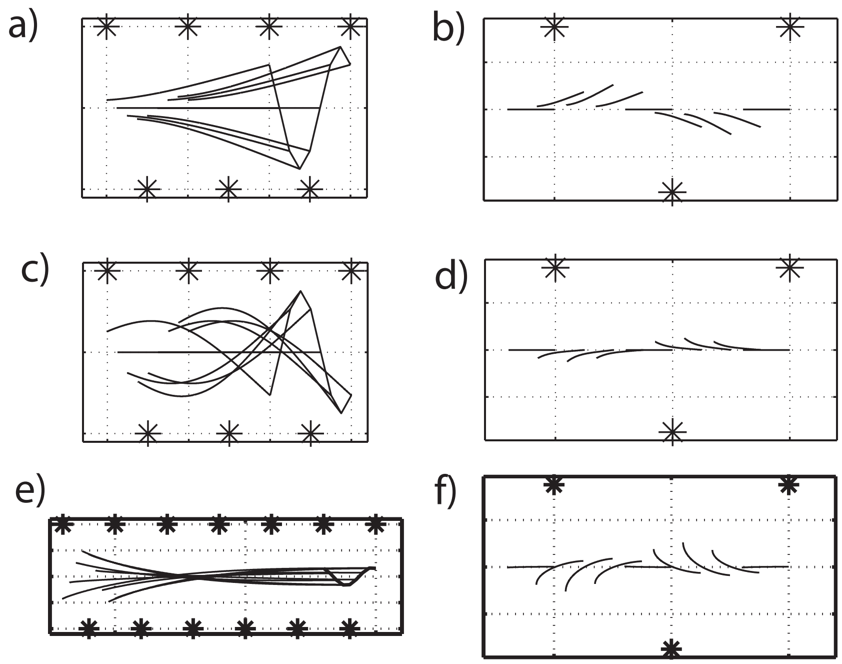

Fig. 2. *Efficiency-maximizing swimming motions for an elastic fin driven at the leading edge (a–d) and a whole body driven all along its length (e, f). Eight snapshots of the fin/body are shown over a period of motion, in a frame which moves with the vortex street. The stiffness and length of the elastic fin are varied as follows: a stiff, long fin (a); a stiff, short fin (b); a more flexible, long fin (c); and a more flexible, short fin (d). A long body is shown in (e), and a short body in (f). (Adapted from [10]).*

problem has a single temporal frequency, which is that of the von Kármán street. The parameter d/l is thus removed from the problem, but the ratio of body length to streamwise vortex separation, L/l, is added. One can again identify body motions which maximize thrust force and efficiency. Some examples of body motions which maximize swimming efficiency are shown in Figure 2.

Two different types of body forcing are considered in Figure 2. In panels a–d, a leading edge heaving and pitching motion is applied to an otherwise passive elastic body, which is a model of a tail fin. Snapshots of the body motions are shown in the frame in which the vortex street is at rest, and the body swims upstream ("slaloms") through the vortex street. Panels a and b show a relatively stiff mode of bending, and panels c and d show a higher bending mode. Panels a and c show bodies which are long (relative to the streamwise vortex spacing) and panels b and d show bodies which are short. In general, the phase of maximum body deflection relative to the passage of the vortices can take on the full range from 0 to

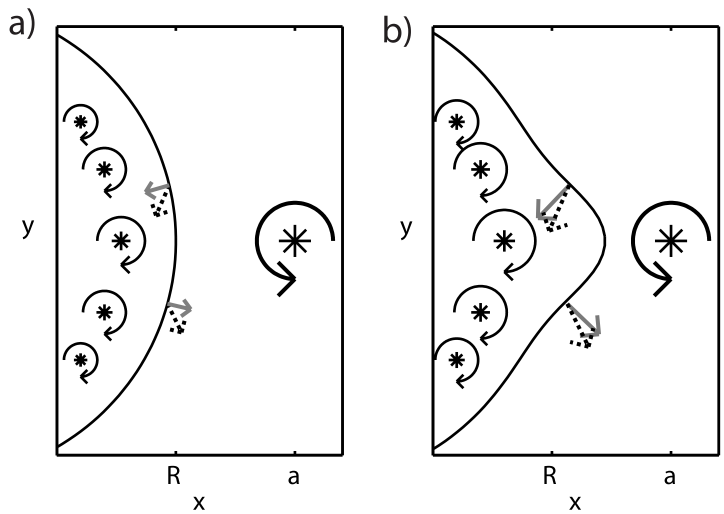

FIG. 3. *a, Point vortex near a rigid circular wall, with induced flow at the wall shown by dashed and gray arrows. b, Point vortex near a flexible circular wall, with a (now larger) induced flow shown by dashed and gray arrows. Adapted from [13].*

2π depending on the parameters L/l and the body stiffness. Panels e and f show efficiency-maximizing motions for a body which is driven all along its length, similarly to an entire fish body. Here the thrust near the leading edge is important, and favors a large body curvature near the leading edge.

Many studies have considered interactions of vortices with rigid bodies relevant to engineering applications, principally aircraft [7, 14]. Interactions between a single vortex and *passive* flexible walls were studied in [13]. Traveling wave solutions were found for two simple wall geometries: an infinite straight line, and a circle, in the undeflected states. In these solutions, the vortex travels parallel to the wall, and the wall flexes outward towards the vortex and the outward bump moves with the vortex in a traveling wave of deflection.

For a circular wall, the force on the wall diverges as the inverse cube of the distance between the point vortex and the wall. The physical mechanism is illustrated in Figure 3. In panel a, a portion of a rigid circular wall near the point vortex (at $x = a$) is shown. The smaller vortices along the inner boundary of the wall represent the bound vortex sheet induced on the wall, which prevents flow from penetrating the wall. The dashed arrows are the flow velocities induced by the point vortex at two points on the wall, and the gray arrows are their components normal to the wall. Panel b shows the same situation but for a flexible wall. The outward deflection of the wall brings it closer to the point vortex. Then the flow induced by the point vortex on the wall (dashed arrows) and their components normal to the wall (gray arrows) are larger. Hence the bound vortex sheet along the wall is stronger, and so is the pressure force on the wall, which leads to a larger deflection, and so on. This self-amplification of the wall deflection leads to the aforementioned inverse-cube force law, and the speed of the point vortex diverges as the inverse fourth power of distance to the flexible wall.

3. Multiple bodies in flows. Another level of complexity is introduced by considering *two* coupled bodies in a flow. Dong and Lu investigated numerically two bodies arranged side-by-side, which undergo a prescribed traveling wave motion [15]. They studied the effect of varying the relative phase between the bodies' traveling waves, and found that in-phase motions can enhance efficiency, while out-of-phase motions can increase the maximum thrust produced. Because the flow is incompressible, large pressures can develop when the bodies move out of phase, which "squeezes" the fluid between them. In-phase motions, by contrast, decrease the relative speed between the body and the ambient fluid. The signature of these effects can be seen in the vortex streets produced by the foils. When the foils move out-of-phase, the vortices are strengthened, whereas for in-phase motions, the vortices are weakened. The resulting change in outward fluid momentum flux causes increased or decreased thrust on the bodies. For the in-phase motion, however, the decreased thrust is accompanied by increased efficiency.

These results are reminiscent of a recent study by Wang and Russell on the coupling of front and hindwing motions in dragonflies [16]. There the dragonfly switches from moving the (essentially rigid) wings in-phase for steady hovering, to out-of-phase, for take-off motions. However, the authors gave a simple interpretation for the increased lift force and efficiency in terms of the relative motion of the wing and the ambient fluid. In each of these cases, the vortex-laden viscous flows surrounding the wings are highly complicated. However, a quasi-steady drag law allows for a simple interpretation of the effect of one wing moving through the wake created by the other.

Other studies have considered coupled motions of two completely passive bodies. Zhu and Peskin used the immersed boundary method to study the effect of the lateral spacing between the flags in a two-dimensional flow [17], inspired by soap film experiments of Zhang *et al.* [18, 19]. They found a transition from out-of-phase flapping, when the flags are far apart, to in-phase flapping when the flags become sufficiently close. This fact connects well with the increase in efficiency noticed by Dong and Lu with in-phase swimming of side-by-side swimmers. The transition in flapping frequencies during these states were studied by Farnell *et al.* [20]. Jia *et al.* studied the same problem in a simpler model, which enabled a more thorough investigation of parameter space [21]. Important parameters are flag displacement-to-length ratio, dimensionless bending energy, and dimensionless flag density. In addition to in-phase and out-of-phase modes, they found more general states which fit into neither category, which they classified as “indefinite” modes. They also investigated different lengths of the flags, which alters the timing and strength of vortex shedding at the trailing edges of the flags through a complex interaction which is not understood on the basis of simple principles.

One of the most interesting problems has been the analysis of propulsion by *coupled* motions of fish fins arranged streamwise. Drucker and Lauder studied the relative motions of the Bluegill sunfish dorsal fin (located atop the body) and caudal (tail) fin [22]. Using a laser light sheet they measured the kinematics of the two fins and the fluid motion in a horizontal cross-section through both fins and the surrounding fluid. They found that vorticity shed from the dorsal fin collides with the caudal fin at different locations along the fin depending on the swimming gait. They found evidence for a constructive interaction between the vorticity shed by the two oscillating fins, which resulted in stronger net vorticity leaving the tail fin. A smaller sweep amplitude and phase advance of 30 degrees were reported for the dorsal fin relative to the caudal fin. Presumably these are among the important parameters characterizing how vorticity from the dorsal fin affects shedding from the tail fin. Due to the complex analysis required to visualize the flow fields, the results were confined to a small set of parameter values.

Ristroph and Zhang studied a related passive system, consisting of a streamwise array of flags in a soap film [23]. As the distance between the second flag’s leading edge and the leading flag’s trailing edge is varied, the drag on both flags can increase and decrease in a nonobvious manner. In particular, they reported an optimum spacing between the flags, leading to a minimum overall drag on the system. The phenomenon is different from “drafting” used to decrease drag in cycling. The amplitude of the flags’ flapping is of the same order as the spacing between them, leading to an unsteady wake with a dominant frequency of oscillation which can only be determined by considering the interaction of the flags and the shed vortex sheets.

We have used a vortex sheet model to gain a more detailed picture of the two-flag system in parameter space [24]. Figure 4 shows snapshots which are representative of the typical dynamics for two flags side-by-side (panels a–c) and in the tandem configuration (panels d–h). For the side-by-side case, as the spacing between the flags is increased, we find a transition from nonperiodic, erratic flapping for closely spaced flags (panel a), to antiphase flapping (panel b), which lies at one end of a range of periodic flapping with monotonic variation of interflag flapping phase with separation distance. In-phase dynamics occur at a separation of about 2.5 flag-lengths (panel c). An experimental study of 2–4 side-by-side flags showed interesting higher-frequency modes of interaction [25]. A linear stability analysis was given by [26].

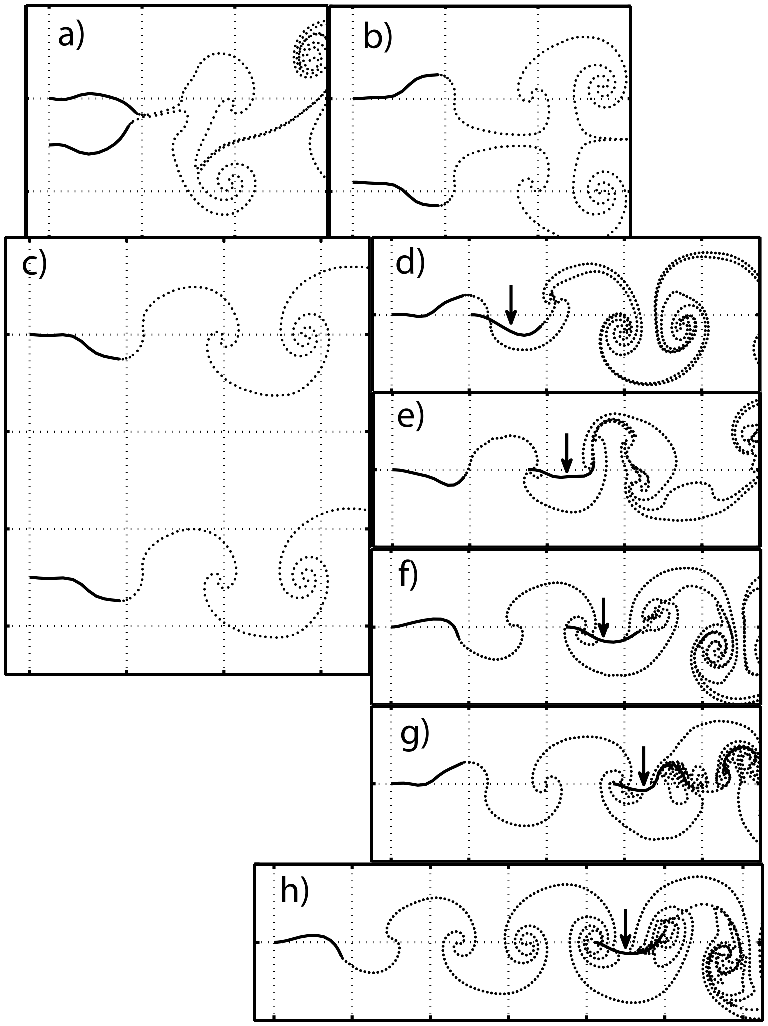

FIG. 4. *Snapshots of a model two flag system in side-by-side (a–c) and tandem (d–h) configurations. The trailing flags in the tandem configurations are indicated by arrows. Adapted from [24].*

The tandem case is somewhat richer, and shows an alternating sequence of synchronous (panels d, f, and h) and asynchronous (panels e and g) flapping states as separation distance increases. The drag force on the follower flag is increased in synchronous flapping, but not in asynchronous flapping. Synchronous flapping seems to occur at flag separations which allow the vortex streets of the leader and follower flag to nearly align, with vortices of the same sign rolling up together. Studies incorporating viscosity found similar results [27, 28].

4. Future directions. We have discussed a set of recent model problems for understanding how bodies interact through flows. One of the future challenges is to move from model problems to an understanding of the fluid dynamical mechanisms at work in a school of fish. Weihs gave a simple model of the forces on individual fish in a school in terms of the relative spacings in a 2D array of fish, with fluid wakes modeled using far-field flows induced by point vortices [29]. More recent studies have modeled multiple swimmers using Hamiltonian systems, with omission or simplification of vortex shedding [30–32].

Biologists have challenged the hydrodynamic importance of schooling, with the observation that three species of schooling fish do not swim in appropriate positions to gain hydrodynamic advantage [33]. The matter remains unresolved, but the hydrodynamic interactions within a fish school are of sufficient intrinsic interest that a more detailed description of the flow in an array of swimmers is desirable [34, 35]. Rapid progress has been made recently on the understanding of collective swimming at low Reynolds numbers [36–39], and similar statistical and mean-field approaches may work well at high Reynolds numbers.

REFERENCES

[1] M.A.R. Koehl. Physical modelling in biomechanics. *Philosophical Transactions of the Royal Society of London. Series B: Biological Sciences*, **358**(1437): 1589, 2003.

[2] J.C. Liao, D.N. Beal, G.V. Lauder, and M.S. Triantafyllou. Fish exploiting vortices decrease muscle activity. *Science*, **302**(5650): 1566–1569, 2003.

[3] J.C. Liao. A review of fish swimming mechanics and behaviour in altered flows. *Philosophical Transactions of the Royal Society B: Biological Sciences*, **362**(1487): 1973, 2007.

[4] J.N. Newman. Swimming of slender fish in a non-uniform velocity field. *The ANZIAM Journal*, **19**(1): 95–111, 1975.

[5] J.O. Dabiri. Renewable fluid dynamic energy derived from aquatic animal locomotion. *Bioinspiration & Biomimetics*, **2**: L1, 2007.

[6] K. Streitlien, G.S. Triantafyllou, and M.S. Triantafyllou. Efficient foil propulsion through vortex control. *AIAA J.*, **34**(11): 2315–2319, 1996.

[7] T.L. Doligalski, C.R. Smith, and J.D.A. Walker. Vortex interactions with walls. *Annual Review of Fluid Mechanics*, **26**(1): 573–616, 1994.

[8] S. Alben. On the swimming of a flexible body in a vortex street. *Journal of Fluid Mechanics*, **635**: 27–45, 2009.

[9] G. Taylor. Analysis of the swimming of microscopic organisms. *Proceedings of the Royal Society of London. Series A, Mathematical and Physical Sciences*, **209**(1099): 447–461, 1951.

[10] S. Alben. Passive and active bodies in vortex-street wakes. *Journal of Fluid Mechanics*, **642**: 95–125, 2009.

[11] J.D. Eldredge and D. Pisani. Passive locomotion of a simple articulated fish-like system in the wake of an obstacle. *Journal of Fluid Mechanics*, **607**: 279–288, 2008.

[12] A. Manela and M.S. Howe. The forced motion of a flag. *Journal of Fluid Mechanics*, **635**: 439–454, 2009.

[13] S. Alben. Interactions between vortices and flexible walls. *International Journal of Non-Linear Mechanics*, **46**: 586–591, 2011.

[14] D. Rockwell. Vortex-body interactions. *Annual review of fluid mechanics*, **30**(1): 199–229, 1998.
[15] G.J. Dong and X.Y. Lu. Characteristics of flow over traveling wavy foils in a side-by-side arrangement. *Physics of Fluids*, **19**: 057107, 2007.
[16] Z.J. Wang and D. Russell. Effect of forewing and hindwing interactions on aerodynamic forces and power in hovering dragonfly flight. *Physical review letters*, **99**(14): 148101, 2007.
[17] L. Zhu and C.S. Peskin. Interaction of two flapping filaments in a flowing soap film. *Phys. Fluids*, **15**: 1954–1960, 2003.
[18] J. Zhang, S. Childress, A. Libchaber, and M. Shelley. Flexible filaments in a flowing soap film as a model for one-dimensional flags in a two-dimensional wind. *Nature*, **408**(6814): 835–839, 2000.
[19] M.J. Shelley and J. Zhang. Flapping and Bending Bodies Interacting with Fluid Flows. *Annual Review of Fluid Mechanics*, **43**(1): 449, 2011.
[20] D.J.J. Farnell, T. David, and D.C. Barton. Coupled states of flapping flags. *J. Fluid. Struct.*, **19**(1): 29–36, 2004.
[21] L.-B. Jia, F. Li, X.-Z. Yin, and X.-Y. Yin. Coupling modes between two flapping filaments. *J. Fluid Mech.*, **581**: 199–220, 2007.
[22] E.G. Drucker and G.V. Lauder. Locomotor function of the dorsal fin in teleost fishes: Experimental analysis of wake forces in sunfish. *J. Exp. Biol.*, **204**(17): 2943–2958, 2001.
[23] L. Ristroph and J. Zhang. Anomalous Hydrodynamic Drafting of Interacting Flapping Flags. *Physical Review Letters*, **101**(19), 2008.
[24] S. Alben. Wake-mediated synchronization and drafting in coupled flags. *Journal of Fluid Mechanics*, **641**: 489–496, 2009.
[25] L. Schouveiler and C. Eloy. Coupled flutter of parallel plates. *Physics of Fluids*, **21**: 081703, 2009.
[26] S. Michelin and S.G. Llewellyn Smith. Linear stability analysis of coupled parallel flexible plates in an axial flow. *Journal of Fluids and Structures*, **25**(7): 1136–1157, 2009.
[27] L. Zhu. Interaction of two tandem deformable bodies in a viscous incompressible flow. *Journal of Fluid Mechanics*, **635**: 455–475, 2009.
[28] S. Kim, W. Huang, and H.J. Sung. Constructive and destructive interaction modes between two tandem flexible flags in viscous flow. *Journal of Fluid Mechanics*, **661**: 511–521, 2010.
[29] D. Weihs. Hydromechanics of fish schooling. *Nature*, **241**(5387): 290–291, 1973.
[30] E. Kanso, J.E. Marsden, C.W. Rowley, and J.B. Melli-Huber. Locomotion of articulated bodies in a perfect fluid. *Journal of Nonlinear Science*, **15**(4): 255–289, 2005.
[31] S.D. Kelly and H. Xiong. Controlled Hydrodynamic Interactions in Schooling Aquatic Locomotion. In *Decision and Control, 2005 and 2005 European Control Conference. CDC-ECC'05. 44th IEEE Conference on*, pp. 3904–3910. IEEE, 2006.
[32] S. Nair and E. Kanso. Hydrodynamically coupled rigid bodies. *Journal of Fluid Mechanics*, **592**: 393–411, 2007.
[33] B.L. Partridge and T.J. Pitcher. Evidence against a hydrodynamic function for fish schools. *Nature*, **279**(5712): 418, 1979.
[34] L.J. Fauci. Interaction of oscillating filaments: A computational study. *Journal of Computational Physics*, **86**(2): 294–313, 1990.
[35] F.E. Fish. Kinematics of ducklings swimming in formation: Consequences of position. *Journal of Experimental Zoology*, **273**(1): 1–11, 1995.
[36] D. Saintillan and M.J. Shelley. Orientational order and instabilities in suspensions of self-locomoting rods. *Physical review letters*, **99**(5): 58102, 2007.
[37] T. Ishikawa and T.J. Pedley. Coherent structures in monolayers of swimming particles. *Physical review letters*, **100**(8): 88103, 2008.

[38] D. Saintillan and M.J. Shelley. Instabilities and pattern formation in active particle suspensions: Kinetic theory and continuum simulations. *Phys. Rev. Lett.*, **100**(17): 178103, 2008.
[39] T.J. Pedley. Collective Behaviour of Swimming Micro-organisms. *Experimental Mechanics*, **50**(9): 1293–1301, 2010.